Electronic structure of PCBM*

Sheng Chun-Qi(盛春荠)[a)b)], Wang Peng(王 鹏)[a)], Shen Ying(沈 影)[a)], Li Yan-Jun(李艳君)[a)], Zhang Wen-Hua(张文华)[c)], Xu Fa-Qiang(徐法强)[c)], Zhu Jun-Fa(朱俊发)[c)], Lai Guo-Qiao(来国桥)[b)], and Li Hong-Nian(李宏年)[a)†]

[a)] *Department of Physics, Zhejiang University, Hangzhou* 310027, *China*

[b)] *Key Laboratory of Organosilicon Chemistry and Material Technology of Ministry of Education, Hangzhou Normal University, Hangzhou* 310012, *China*

[c)] *National Synchrotron Radiation Laboratory, University of Science and Technology of China, Hefei* 230029, *China*

(Received 20 July 2011; revised manuscript received 5 September 2011)

We have studied the electronic structure of [6,6]-phenyl-C_{61}-butyric-acid-methyl-ester (PCBM) using synchrotron radiation photoelectron spectroscopy (PES) measurements and first-principles calculations. The PES spectrum of the entire occupied valence band is reported, which exhibits abundant spectral features from the Fermi level to $\sim$ 24 eV binding energy. All the spectral features are broadened as compared with the cases of C_{60}. The reasons for the broadening are analysed by comparing the experimental data with the calculated energy levels and density of states. Special attention is paid to the analysis of the C_{60} highest occupied molecular orbital (HOMO)-1 derived states, which can play a crucial role in the bonding at the interfaces of PCBM/polymer blenders or PCBM/electrodes. Besides the well-known energy level splitting of the C_{60} backbone caused by the lowered symmetry, C 2p states from the side chain mix or hybridize with the molecular orbitals of parent C_{60}. The contribution of the O 2p states can substantially modify the PES spectrum.

Keywords: [6,6]-phenyl-C_{61}-butyric-acid-methyl-ester (PCBM), electronic structure, photoelectron spectroscopy, density functional theory

PACS: 71.20.Tx, 31.15.ae **DOI:** 10.1088/1674-1056/21/1/017102

1. Introduction

The C_{60} derivative, [6,6]-phenyl-C_{61}-butyric-acid-methyl-ester (PCBM), has been widely used as an electron acceptor in polymer solar cells. However, for commercial applications, further increase of the power conversion efficiency of the solar cells is needed. Aiming toward this goal, much effort has been dedicated to the electronic structure of PCBM, including first-principles calculations[1−7] and PES measurements.[1,8−15] These works provided important information about the electronic states in the vicinity of the highest occupied molecular orbital (HOMO) and the lowest unoccupied molecular orbital (LUMO), but knowledge of the entire occupied valence band is absent. The influence of the phenyl-butyric-acid-methyl-ester side chain on the electronic states of the parent C_{60}, is far from thoroughly understood.

In the present work, we measure the entire occupied valence band on a PCBM film using the synchrotron radiation PES technique. First-principles calculations of the PCBM molecule are carried out to interpret the measured spectra. Special attention is paid to the C_{60} HOMO-1 derived states because of two reasons. First, these states have not been studied in detail in the literature. Second, these states can play a crucial role in the bonding at the interfaces of PCBM/polymer blenders or PCBM/electrodes, and thus affect the performance of the solar cells.

2. Experiment and calculation details

Sample preparation and measurements were performed at the Surface Science Station of the National Synchrotron Radiation Laboratory of China. The base pressure was 6×10^{-11} mbar (1 mbar = 100 Pa). Commercial PCBM was sublimed from a Ta boat located at $\sim$ 10 cm from a Si:H(111) substrate. The sub-

*Project supported by the National Natural Science Foundation of China (Grant No. 11079028) and the National Synchrotron Radiation Laboratory of China.

†Corresponding author. E-mail: phylihn@public.zju.edu.cn

© 2012 Chinese Physical Society and IOP Publishing Ltd

strate was transferred into vacuum chamber immediately after HF acid etching and followed by degassing at 300°C for 1 h. The PCBM powder was thoroughly degassed and then evaporated onto the Si:H(111) substrate to form a solid film. The thickness of the film was not quantitatively estimated. What we can say is that the film was rather thick, since the sample holder became light yellow by close inspection.

An angle-resolved electron energy analyzer was used to record the photoelectrons at an emission angle of 23° with respect to the sample normal. The total energy resolution was 0.1–0.2 eV with increasing photon energies. We adopted the photon energy of 60.9 eV to measure the entire valence band in a large binding energy (BE) range from the Fermi level to $\sim$ 29 eV. Spectra in a smaller BE range were recorded with some different photon energies.

The first principle calculations were performed by using the DMol^3 package[16,17] based on the density functional theory (DFT). The functional adopted in this work is the BLYP[18,19] generalized gradient approximation (GGA) functional. All-electron calculations were performed with the double numerical basis sets plus polarization function (DNP). The geometry was optimized without symmetry constraints. The criteria for convergence were 1×10^{-5} Ha (1 Ha = $4.35974417(75) \times 10^{-18}$ J) for energy, 2×10^{-3} Ha/Å for force, 5×10^{-3} Å for displacement, and 3.7 Å for the orbital cutoffs. The self-consistent field procedures were carried out with a convergence criterion of 10^{-6} Ha for the energy and electron density.

3. Results and discussion

Figure 1 shows the entire occupied valence band measured with the photon energy of 60.9 eV. For convenience, we label the three lowest BE features as A–C. The BE feature A is 2.50 eV, and the valence band extends to $\sim$ 24 eV BE. A spectrum of C_{60} film[20] measured with $h\upsilon$ = 61.9 eV is also shown for comparison. The main difference between the two spectra is that the dips between adjacent spectral features of PCBM are very shallow as compared with C_{60}. The broadening of the spectral features is, of course, caused by the phenyl-butyric-acid-methyl-ester side chain. In particular, there should be three channels of the side chain to modify the spectrum of C_{60} backbone. First, the side chain lifts the degeneracies of the energy levels of C_{60}. Second, some electronic states of the side chain mix with the states of the backbone, and have their own photoelectron signal. The last is orbital hybridizations between the backbone and the side chain. The first channel has been addressed in almost all the published works.[1−15] However, very little is known about the other channels, which will be discussed based on the following DFT results.

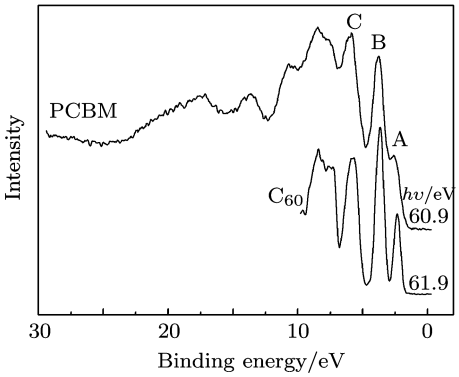


Fig. 1. The entire occupied valence band of PCBM film measured by PES with the photon energy of 60.9 eV. A spectrum of C_{60} film (from Ref. [20]) is also shown for comparison.

Figure 2 exhibits the optimized geometric structure of PCBM and some calculated energy levels. The energy gap between LUMO and HOMO is 1.496 eV, smaller than the gap of 1.666 eV for C_{60}. The five levels from HOMO to HOMO-4 of PCBM can be easily understood by the 5-fold degenerated HOMO of the parent C_{60} which splits in the environment of PCBM. Analogously, the three levels from LUMO to LUMO+2 of PCBM are derived from the 3-fold degenerated LUMO of C_{60}. These observations coincide with the reported results[1−7] that the levels in the vicinity of the HOMO and LUMO of PCBM are almost completely C_{60} backbone derived states. The influence (except the level splitting) of the side chain is mainly reflected on deeper levels. The thirteen levels from HOMO-5 to HOMO-17 of PCBM should correspond to the HOMO-1 (g_g and h_g levels) of C_{60}. However, the HOMO-1 of C_{60} can at most split into nine levels. The extra levels are either the states of the side chain or the hybridizing states.

The calculated electronic states of the entire occupied and some unoccupied valence orbitals are presented by the density of states (DOS) in Fig. 3. Besides the total density of states (TDOS), we also show the local density of states (LDOS) projected onto different constituents of the molecule and the partial density of states (PDOS) projected onto different angular momenta. From Fig. 3, the interaction between the side chain and the C_{60} backbone can be deduced.

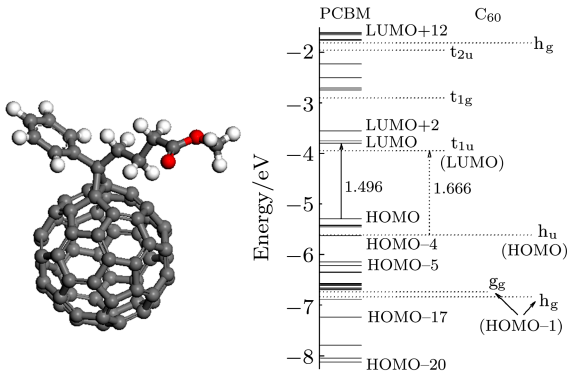


Fig. 2. (colour online) (a) Geometric structure of PCBM. The grey, red and white balls represent C, O and H atoms, respectively. (b) The calculated energy level diagrams of PCBM (solid horizontal lines) and C_{60} (dotted horizontal lines). The energy levels of C_{60} were calculated by using the same method as for PCBM, and the irreducible representations of the I_h point groups are indicated for each level. The lengths of the horizontal lines are proportional to the degeneracies of the levels. Note that some levels are too close in energy to be separated in the figure.

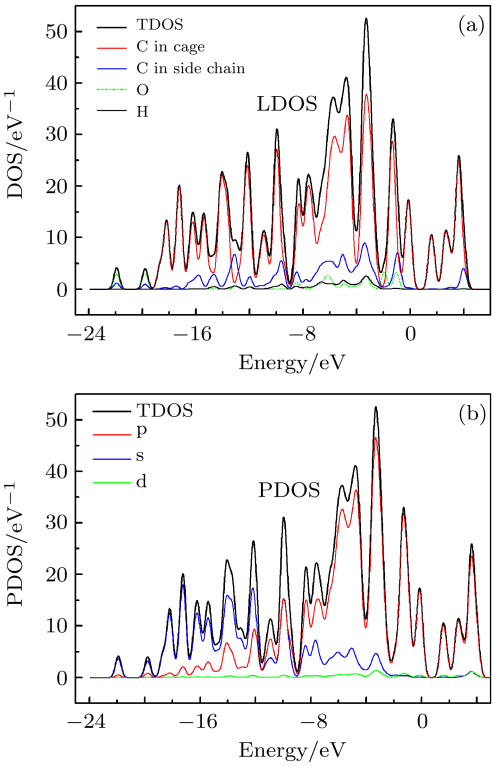


Fig. 3. (colour online) TDOS, LDOS (a) and PDOS (b) of PCBM. The zero of the energy axis corresponds to the HOMO position. The DOSs were generated by using the DMol^3 package with a smearing width of 0.2 eV.

Figure 4(a) shows the comparison of the occupied part of the TDOS with the experimental data, in which a spectrum recorded with $h\upsilon = 40.8$ eV is also presented because it exhibits more clear separation between features A and B. The energy of the TDOS

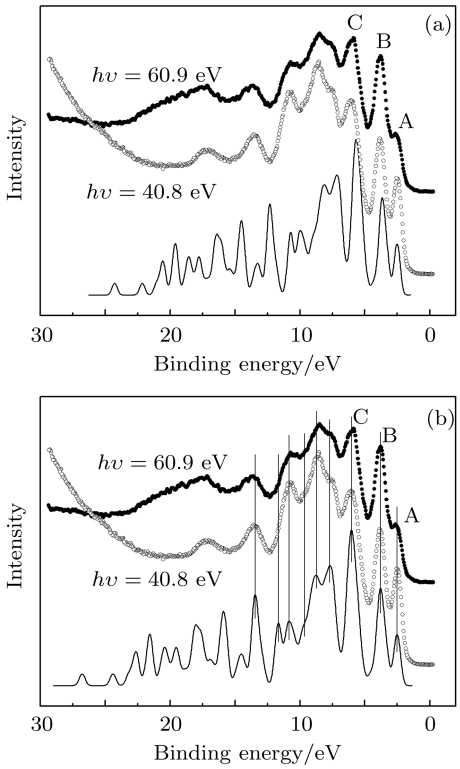


Fig. 4. (a) Comparison between the experimental data (filled and open circles) and the theoretical TDOS. (b) Comparison between the experimental data and the remedied theoretical TDOS (multiplied by a coefficient of 1.115 in energy scale). Only the occupied part of the TDOS is shown.

is changed to be positive to match the tendency of PES (giving the binding energies as positive numbers), and shifted to make the TDOS coincide with feature A. Despite the general coincidence of Fig. 4(a), the energy intervals between the TDOS peaks are shrunken as compared with the experimental data. This disagreement is a universal shortcoming of DFT calculations. All published theoretical DOSs of fullerene molecules exhibit this disagreement. Fortunately, we found that a simple remedy of multiplying the energy scale of the calculated results by a coefficient can eliminate the disagreement.[21,22] Figure 4(b) shows the comparison of the experimental data with the remedied TDOS whose energy scale has been multiplied by a coefficient of 1.115. After the energy correction, the TDOS coincides with the spectra very well (especially for the 2p-dominated states from the Fermi level to ∼14 eV BE, as indicated by the vertical lines). According to Fig. 4(b), the valence band extends to ∼ 27 eV BE. However, the bottom of the valence band is the O 2s derived states (see Fig. 3), which cannot be measured by the PES due to the small DOS and their small photoionization cross-section at $h\upsilon = 60.9$ eV.[23] For the spectrum of $h\upsilon = 40.8$ eV,

all the higher BE (greater than ∼ 18 eV) signals of the sample are embedded in the secondary electron background. The good coincidence between the TDOS of PCBM molecule and the spectra of the solid film reveals that the interaction between the molecules is weak.

Based on the good coincidence of Fig. 4(b), we are confident of analysing the effect of the side chain on the electronic structure of PCBM in more detail by utilizing the LDOS and PDOS in Fig. 3. Among the abundant PES features, feature B has a substantial contribution from the side chain (see Fig. 3(a)). This feature comprises the HOMO-1 derived states of C_{60} (see Fig. 2(b)). The HOMO-1 states of C_{60} are the outermost (in spatial distribution) states, which play an crucial role in the bonding of solid C_{60} and C_{60}/metal interfaces.[24,25] Through participating in the bonding, these states can indirectly affect the energy positions of the LUMO and HOMO of PCBM in its blends with polymers or in the PCBM/electrode interfaces, and then affect the performance of the solar cells. However, it seems that the significance of feature B was not realized by the reported works.[1−15] We thus try to obtain a thorough understanding of the structure of feature B. Figure 5 puts together feature B (measured with $h\upsilon$ = 40.8 eV) and its calculated counterparts (energy levels, TDOS and LDOS). The LDOS and the energy levels have been shifted and corrected the same as in Fig. 4(b). Different from that in Figs. 3 and 4, the DOSs in Fig. 5 are plotted with a rather small smearing width of 0.04 eV to reveal the constituents of the electronic states. From Figs. 5 and 3(b), it is clear that the photoelectron signal around the center of feature B is from the C 2p of C_{60} backbone with negligible contribution from the side chain. In particular, the C 2p states around the center of feature B are the eight energy levels split from the HOMO-1 of parent C_{60}. The states of one remaining level of the HOMO-1 of C_{60} hybridize with the C 2p states of the side chain, distributed between 3.2 and 3.6 eV BE. The O 2p states are distributed at the two sides of feature B, at ∼ 3.5 eV and ∼ 4.5 eV BE. The conclusions of Fig. 5 are meaningful not only for PCBM itself but also for optimizing the performance of PCBM-based solar cells. Since the PES technique is a powerful tool in the study of the electronic states of PCBM/polymer blenders[10,12,14,15] and PCBM/electrode interfaces,[9] we predict that future PES studies should measure feature B to study the bonding and the related energy level alignments. Then the conclusions of Fig. 5 are rather instructive.

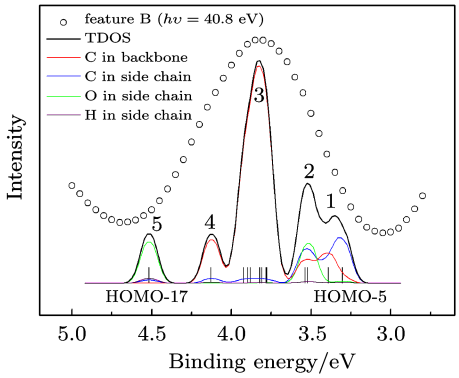


Fig. 5. (colour online) Illustration of the constituents of the electronic states giving rise to the photoelectrons of feature B. The DOSs were generated with a small smearing width of 0.04 eV. The multiplying coefficient of 1.115 has been applied to the energy scales of the DOSs and the energy levels.

At the end of this paper, we show in Fig. 6 more spectra measured with different photon energies. Figure 6 exhibits shallower and shallower dips between features A–C with increasing photon energies. This is simply a verification of the conclusions of Fig. 5.

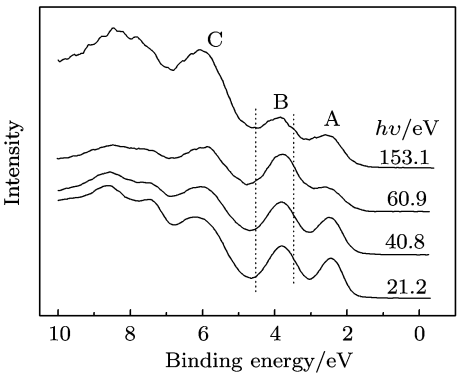


Fig. 6. Photoelectron spectra of PCBM film measured with four different photon energies. The vertical dotted lines indicate the positions of the O 2p states. The spectral lines are normalized to the height of feature B.

According to Fig. 5, one important reason for the broadening of feature B is the O 2p states distributed at the two sides. The electron occupation of feature B is 26 according to the corresponding 13 energy levels, among which the number of O 2p electrons is near 4. At the photon energy of 21.2 eV, the ratio of photoionization cross section between O 2p and C 2p is ∼ 0.9 (per electron),[23] and the contribution of the O 2p electrons to the spectrum is minor but non-negligible. The ratio increases monotonically with photon energies.[23] At the photon energy of 153.1 eV, the ratio is ∼ 4.3.[23] That is to say, the photoelectron intensity of the O 2p electrons at the higher BE side of

feature B is approximately equivalent to that of eight C 2p electrons, and thus the dip between features B and C is rather shallow in the spectrum measured with $h\upsilon = 153.1$ eV. In addition to verifying some conclusions of the present work, Fig. 6 also provides a guideline for future PES works about selecting appropriate photon energy for specific purposes.

4. Conclusions

The entire occupied valence band of PCBM extends to ~ 27 eV BE, which can be observed by photoelectron spectroscopy, except for the O 2s states at the bottom of the valence band. DFT results, after a simple remedy, coincide with the PES data very well. The detail is revealed for the contribution of the side chain to the electronic states of feature B. Eight levels located around the center of this feature are from the splitting of C_{60} HOMO-1. The side chain contributes to this feature by hybridizing with the molecular orbitals of C_{60} at the low BE side and arranging O 2p states at both sides. The photon-energy-dependent PES data further verifies the conclusions. The detail of the entire valence band, if necessary, can be acquired straightforwardly from the LDOS and PDOS reported in this article.

References

[1] Akaike K, Kanai K, Yoshida H, Tsutsumi J, Nishi T, Sato N, Ouchi Y and Seki K 2008 *J. Appl. Phys.* **104** 023710

[2] Nápoles-Duarte J M, Reyes-Reyes M, Ricardo-Chavez J L, Garibay-Alonso R and López-Sandoval R 2008 *Phys. Rev.* B **78** 035425

[3] Morvillo P and Bobeico E 2008 *Sol. Energy Mater. Sol. Cells* **92** 1192

[4] Zhang C R, Chen H S, Chen Y H, Wei Z Q and Pu Z S 2008 *Acta Phys. Chim. Sin.* **24** 353

[5] Zhang Z, Han P, Liu X, Zhao J, Jia H, Zeng F and Xu B 2008 *J. Phys. Chem.* C **112** 19158

[6] Bazylewski P F, Kim K H, Forrest J L, Tada H, Choi D H and Chang G S 2011 *Chem. Phys. Lett.* **508** 90

[7] Schwenn P E, Burn P L and Powell B J 2011 *Org. Electron.* **12** 394

[8] Kanai K, Akaike K, Koyasu K, Sakai K, Nishi T, Kamizuru Y, Nishi T, Ouchi Y and Seki K 2009 *Appl. Phys.* A **95** 309

[9] Akaike K, Kanai K, Ouchi Y and Seki K 2009 *Appl. Phys. Lett.* **94** 043309

[10] Akaike K, Kanai K, Ouchi Y and Seki K 2009 *Appl. Phys. Lett.* **95** 113306

[11] Cho S, Seo J H, Lee K and Heeger A J 2009 *Adv. Func. Mat.* **19** 1459

[12] Xu Z, Chen L M, Chen M H, Li G and Yang Y 2009 *Appl. Phys. Lett.* **95** 013301

[13] Guan Z L, Kim J B, Wang H, Jaye C, Fischer D A, Loo Y L and Kahn A 2010 *Org. Electron.* **11** 1779

[14] Tsoi W C, Spencer S J, Yang L, Ballantyne A M, Nicholson P G, Turnbull A, Shard A G, Murphy C E, Bradley D D C, Nelson J and Kim J S 2011 *Macromolecules* **44** 2944

[15] Vaynzof Y, Kabra D, Zhao L, Chua L L, Steiner U and Friend R H 2011 *ACS Nano* **5** 329

[16] Delley B 1990 *J. Chem. Phys.* **92** 508

[17] Delley B 2000 *J. Chem. Phys.* **113** 7756

[18] Becke A D 1988 *J. Chem. Phys.* **88** 1053

[19] Lee C, Yang W and Parr R G 1988 *Phys. Rev.* B **37** 785

[20] Wang X X, Xu Y B, Li H N, Zhang W H and Xu F Q 2008 *J. Electron Spectrosc. Relat. Phenom.* **165** 20

[21] Li H N, Yang H, Wang X X, Ni J F, Wang P, Meng L, Wang X B, Kurash I, Qian H J, Wang J O and Liu Z Y 2009 *J. Phys.: Condens. Matter* **21** 265502

[22] Li Y J, Wang P, Ni J F, Meng L, Wang X B, Sheng C Q, Li H N, Zhang W H, Xu Y, Xu F Q and Zhu J F 2011 *J. Electron Spectrosc. Relat. Phenom.* **184** 414

[23] Yeh J J and Lindau I 1985 *Atomic Subshell Photoionization Cross Section and Asymmetry Parameters:* $1 \leq Z \leq 103$ (New York: Academic) pp. 7–11

[24] Satpathy S, Antropov V P, Andersen O K, Jepsen O, Gunnarsson O and Liechtenstein A I 1992 *Phys. Rev.* B **46** 1773

[25] Li H N, Wang X X, He S L, Ibrahim K, Qian H J, Su R, Zhong J, Abbas M I and Hong C H 2005 *Surf. Sci.* **586** 65